

## Mesosphere/lower thermosphere prevailing wind model

Yu. Portnyagin<sup>a,\*</sup>, T. Solovjova<sup>a</sup>, E. Merzlyakov<sup>a</sup>, J. Forbes<sup>b</sup>, S. Palo<sup>b</sup>, D. Ortland<sup>c</sup>,  
W. Hocking<sup>d</sup>, J. MacDougall<sup>d</sup>, T. Thayaparan<sup>e</sup>, A. Manson<sup>f</sup>, C. Meek<sup>f</sup>, P. Hoffmann<sup>g</sup>,  
W. Singer<sup>g</sup>, N. Mitchell<sup>h</sup>, D. Pancheva<sup>h</sup>, K. Igarashi<sup>i</sup>, Y. Murayama<sup>i</sup>, Ch. Jacobi<sup>j</sup>,  
D. Kuerschner<sup>j</sup>, A. Fahrutdinova<sup>k</sup>, D. Korotyshkin<sup>k</sup>, R. Clark<sup>l</sup>, M. Taylor<sup>m</sup>,  
S. Franke<sup>n</sup>, D. Fritts<sup>o</sup>, T. Tsuda<sup>p</sup>, T. Nakamura<sup>p</sup>, S. Gurubaran<sup>q</sup>, R. Rajaram<sup>q</sup>,  
R. Vincent<sup>r</sup>, S. Kovalam<sup>r</sup>, P. Batista<sup>s</sup>, G. Poole<sup>t</sup>, S. Malinga<sup>t</sup>, G. Fraser<sup>u</sup>,  
D. Murphy<sup>v</sup>, D. Riggini<sup>o</sup>, T. Aso<sup>w</sup>, M. Tsutsumi<sup>w</sup>

<sup>a</sup> Institute for Experimental Meteorology, Lenin str. 82, Obninsk 249038, Russia

<sup>b</sup> University of Colorado Aerospace Engineering Sciences, UCB 429, Boulder, CO 80309-0429, USA

<sup>c</sup> North West Research Associates, 14508 NE, 20th Street, Bellevue, WA 98007-3713, USA

<sup>d</sup> Department of Physics, Physics and Astronomy Building, University of Western Ontario, London, Ont., Canada N6A 3K7

<sup>e</sup> Defense Research Establishment Ottawa Surface Radar, 3701 Carling Avenue, Ottawa, Ont., Canada K1A 0Z4

<sup>f</sup> Institute Space and Atmospheric Studies, University of Saskatchewan, 116 Science Place Saskatoon, Saskatchewan, Canada S7N 5E2

<sup>g</sup> Leibniz-Institute of Atmospheric Physics, Rostock University, Schloss-Strasse 6, Kuehlungsborn D-18225, Germany

<sup>h</sup> University of Bath Electronic and Electrical Engineering, Claverton Down Bath BA2 7AY, UK

<sup>i</sup> Communications Research Laboratory, Int'l. Arctic Environment Res., Team 4-2-1, Nukui-kita-Machi Kogane-shii, Tokyo 184-8795, Japan

<sup>j</sup> Leipzig University Institute for Meteorology, Stephanstr. 3, Leipzig D-04103, Germany

<sup>k</sup> Radiophysics Department, Department of Physics, Kazan University, Kremlevskaiastr. 18, Kazan 420008, Russia

<sup>l</sup> Electrical and Computer Engineering, University of New Hampshire, Kingsbury, Durham, NH 03824, USA

<sup>m</sup> Utah State University, CASS 4415 Old Main Hill, Logon, UT 84322-4415, USA

<sup>n</sup> University of Illinois Space Science and Remote Sensing Laboratory, 1308 W. Main Street, Urbana, IL 61801, USA

<sup>o</sup> Colorado Research Associates, 3380 Mitchell Lane, Boulder, CO 80301, USA

<sup>p</sup> Kyoto University, Radio Atmospheric Science Center, Uji, Kyoto 611-0011, Japan

<sup>q</sup> Equatorial Geophysical Research Laboratory, Indian Institute of Geomagnetism, Krishnapuram, Tirunelveli, TN 627 011, India

<sup>r</sup> Physics and Maths Physics, University of Adelaide, Adelaide 5005, Australia

<sup>s</sup> INPE Aeronomy Division, C.P. 515, Sao Jose dos Campos, SP 12200, Brazil

<sup>t</sup> Department of Physics and Electronics, Rhodes University, P.O. Box 94, Grahamstown 6140, Republic of South Africa

<sup>u</sup> Department of Physics and Astronomy, University of Canterbury, Private Bag 4800, Christchurch, New Zealand

<sup>v</sup> Atmospheric and Space Physics, Australian Antarctic Division, Channel Highway Kingston, Tasmania 7050, Australia

<sup>w</sup> National Institute of Polar Research, 9-10 Kaga, 1 Chome Itabashi-Ku, Tokyo 173-8515, Japan

Received 19 October 2002; received in revised form 1 April 2003; accepted 2 April 2003

### Abstract

The mesosphere/lower thermosphere (MLT) wind data from the 46 ground-based (GB) MF and meteor radar (MR) stations, located at the different latitudes over the globe, and the space-based (SB) HRDI data were used for constructing of the empirical global climatic 2-D prevailing wind model at 80–100 km heights for all months of the year. The main data set is obtained during 1990–2001 period. It is shown that the three datasets (MF, MR, HRDI) are mainly well correlated. However, a certain systematic bias between the GB and SB data at 96 km exists, as well as that between the MF and MR data higher 88 km. Simple correction factors are proposed to minimize these biases. The 2-D distant-weighted least-square interpolation procedure for some arbitrary

\* Corresponding author.

E-mail address: [yportgin@typhoon.obninsk.org](mailto:yportgin@typhoon.obninsk.org) (Y. Portnyagin).

collection of points was used for drawing model contour plots. The model is available in the computer readable form and may be used for construction of the new CIRA model.

© 2004 COSPAR. Published by Elsevier Ltd. All rights reserved.

*Keywords:* Mesosphere/lower thermosphere; Prevailing wind model

## 1. Introduction

There are relatively few global empirical climatic 2-D models of the mesosphere/lower thermosphere (MLT) prevailing winds. The most recent review of these models is given by Portnyagin and Solovjova (2002). All of the existing models are constructed using assimilation of the some ground-based radar data or the space-based (UARS) data without their combination. Herewith the radar data are sporadically distributed over different observational campaigns during different years and even decades. Meanwhile, in frame of many international projects (PSMOS, in particular) the last

decade was marked by unprecedented measurement activity at the old and new radar stations, well distributed over the globe. And namely in this decade the UARS MLT wind measurements were carried out. Ground-based (GB) instruments have the obvious advantage of good time resolution, but are distributed sparsely over the globe. Space-based (SB) measurements offer global coverage, but poor time resolution at various points fixed on the earth. In order to deconvolve unambiguously the spatial and temporal characteristics of the dynamically evolving MLT circulation, it is becoming increasingly evident that the SB and GB measurements need to be assimilated together in some

Table 1

	Station	Location	Observed period	Equipment	Height limits
1	<i>Heiss isl.</i>	80.5°N, 58°N,	1965–1981	MR	88–90
2	<b>Resolute Bay</b>	75°N, 95°W	1997–2001	VHF(meteors)	<b>82–98</b>
3	<b>Dixon Island</b>	72.5N, 80.5E	1999–2001	MR	88
4	<b>Tromse</b>	70N, 19E	1994–2000	MF	70–97
5	<b>Andenes</b>	69.3N, 16.0E	1999–2001	MF	70–98
6	<b>Esrang</b>	68N, 21E	1999–2001	MR	81–97
7	Kiruna	68N, 20E	1974–1975	MR	70–100
8	<b>Poker Flat</b>	65N,147W	1998–2000	MF	50–108
9	<b>Kazan</b>	56N, 49E	1986–2000	MR	82–100
10	<i>Obninsk</i>	55N, 37E	1991–2001	MR	90
11	<b>Juliusruh</b>	54.6N, 13.4E	1990–2001; 2000–2001	MF; MR	74–96, 5; 82–98
12	<b>UK*</b>	53.3N, 3.8W	1988–2001	MR	90
13	<b>Collm</b>	52N, 15E	1983–2001	LF	82.5–105
14	<b>Saskatoon</b>	52N, 107W	1991–2000	MF	70–97
15	<i>Khabarovsk</i>	49N, 135E	1975–1985	MR	90
16	<i>Volgograd</i>	49N, 44E	1983–1991	MR	90
17	Garchy	47N, 3E	1970–1976	MR	78–102
18	Monpazier	45N, 1E	1975–1980	MR	80–100
19	<b>Wakkanai</b>	45.4N, 142E	1997–2000	MF	60–98
20	<b>London</b>	43N, 81W	1994–1997; 1994–2000	MF; MR	82–98; 82–98
21	<b>Durham</b>	43N, 71W	1993,1994,1999	MR	95
22	<b>Yambol</b>	42.5N, 26.5E	1989–1993	MR	90
23	<b>Bear Lake</b>	42N, 111.4W	2000–2001		82–98
24	<b>Urbana</b>	40N, 88W	1991–2000	MF	60–99
25	<b>Shigaraki</b>	35N, 136E	1991–1999	MU	82–99
26	<b>Albuquerque, New Mexico</b>	35N, 107W	1998–2001	MR	82–98
27	<b>Yamagawa</b>	31.2N, 130.6E	1996–2000	MF	60–98
28	Kauai	22N, 160W	1991–1992	MF	82–98
29	Punta Borinquen	18N, 67W	1977–1978	MR	80–100
30	<b>Tirunelveli</b>	8.7N, 77.8E	1992–1999	MF	70–98
31	<i>Mogadisho</i>	2N, 45E	1968–1970	MR	90
32	<b>Christmas isl.</b>	2N, 158W	1990–1997	MF	78–98
33	<b>Jakarta</b>	6S, 107E	1992–1995	MR	80–100
34	Townsville	20S, 147E	1978–1980	MF	70–98
35	<b>Cachoeira Paulista</b>	22.7S, 45.2W	1999–2001	MR	80–100
36	<b>Grahamstown</b>	33.3S, 26.5E	1987–1993	MR	90

Table 1 (continued)

	Station	Location	Observed period	Equipment	Height limits
37	<b>Adelaide</b>	<b>35S, 138E</b>	1991–1997	MF	78–98
38	<b>Christchurch</b>	<b>44S, 173E</b>	1996,1997	MF	82.5–100
39	<b>Mawson</b>	<b>68S, 63E</b>	1984–1987	MF	80–110
40	<i>Molodezhnaya st.</i>	<i>68S, 45 E</i>	1961–1991	MR	90
41	<b>Davis</b>	<b>68.6S, 167E</b>	1999–2000	MF	70–98
42	<b>Rothera</b>	<b>67.57S, 68.13W</b>	1997–1998	MF	60–98
43	<b>Syowa</b>	<b>69S, 39.6E</b>	1999–2001	MF	60–98
44	McMurdo	77.85S, 166.6E	1996–1998	MF	70–98
45	Scott Base	78S, 167E	1982–1984	MF	81–97
46	<i>Amundsen Scott</i>	<i>90S</i>	1995–1996	MR	90

Some comments in Table 1: the bold letters show the main set of the stations for the period 1990–2001, which would be the core of the model. The italic letters denote that the station is without height determination. The data from the stations earlier than 1990 would be also used, but with lower weighting and only in the case when they did not contradict to the more new data. These data would help to see at the climatic trends and year-to-year wind variability as well. UK\* – The radar has moved around a little, but not much. Here are the details: Sheffield (53°23'N, 1°27'W) – January 1988–May 1995; Rutherford Laboratory (51°34'N, 1°19'W) – March 1995–April 1998; Castle Eaton (51°40'N, 1°47'W) – April 1998–December 2000.

way. This requires the SB and GB measurements to consistently represent the dynamical circulation, or that they be intercalibrated so that consistency is achieved. So, it is right time now to develop an updated comprehensive global prevailing model using both the ground-based and space-based datasets.

## 2. Datasets

The most reliable ground-based MLT wind measurements are carried out with help of the meteor radars and the MF ones. The list of the observational sites, their geographical location and information about measurement periods is given in Table 1. As can be seen from Table 1, the main bulk of the data comprise the period 1990–2000. The datasets for other periods would be used as complimentary ones. The space-based data utilized here consist of horizontal wind measurements from the HRDI instrument (Hays et al., 1993) on board the Upper Atmosphere Research Satellite (UARS). The data are the Level 3AL wind data distributed by the NASA Goddard Space Flight Center. These dataset cover the period since December 1991–January 1999. The height level near 96 km was selected because around this altitude both daytime and nighttime observations are available, thus permitting effective removal of the tidal components from the measurement results. Due to the local time, orbital and viewing constraints of the HRDI instrument we limited the latitude coverage of the space-based data to within 50°N–50°S latitudinal belt.

## 3. Method of the model construction

For constructing of the model the HRDI data were preliminary evaluated in the following manner. At each 10° by 10° (latitude/longitude) area or cell, time se-

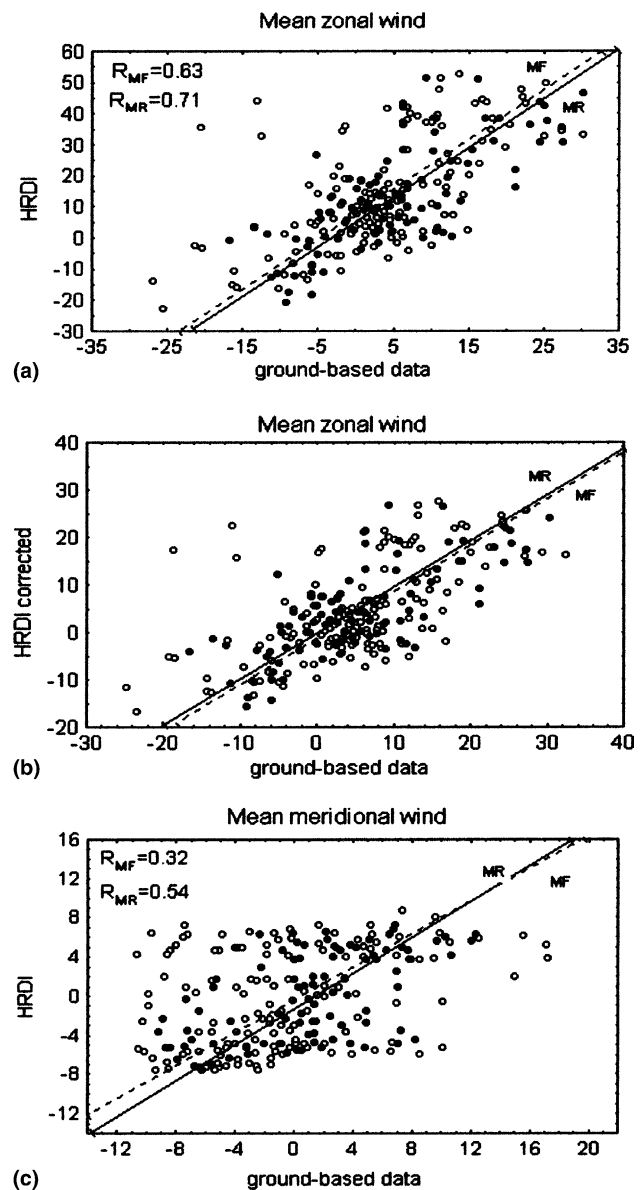


Fig. 1. Scatter diagrams for HRDI/radar comparison for monthly mean winds: ○ – MF (dashed line); ● – MR (solid line).

quences of the HRDI winds for the each month of all years of observations were reformed into 24 h mean-days only according to their time (in UT) of day. This procedure was repeated with a  $5^\circ$  shift along the latitude and longitude to provide some additional smoothing of the data. As a result, the hourly mean climatic wind values were obtained for each  $5^\circ$  by  $5^\circ$  bin for each month. These values for each hour of day were subjected to the 2-D distant-weighted least-square interpolation procedure for some arbitrary collection of points (McLane, 1972). As a result for each wind component (zonal and meridional) 24 sets of the wind data for each

knot centered in the  $5^\circ$  by  $5^\circ$  (latitude/longitude) bin were calculated. After that harmonic fitting was applied to the data for each knot (node) to obtain the daily mean (prevailing) winds and the amplitudes and phases of the 12 and 24 h tides. Then, the wind data for the each  $5^\circ$  longitudinal belt were subjected to the harmonic analysis over longitude and the parameters of the planetary waves with the zonal wavenumbers  $s = 0, \pm 1, \pm 2, \pm 3$  and  $\pm 4$  were found. The only zonally averaged winds ( $s = 0$ ) were used for our following analysis. Additionally (see Section 5) the zonally averaged monthly mean meridional winds were smoothed using

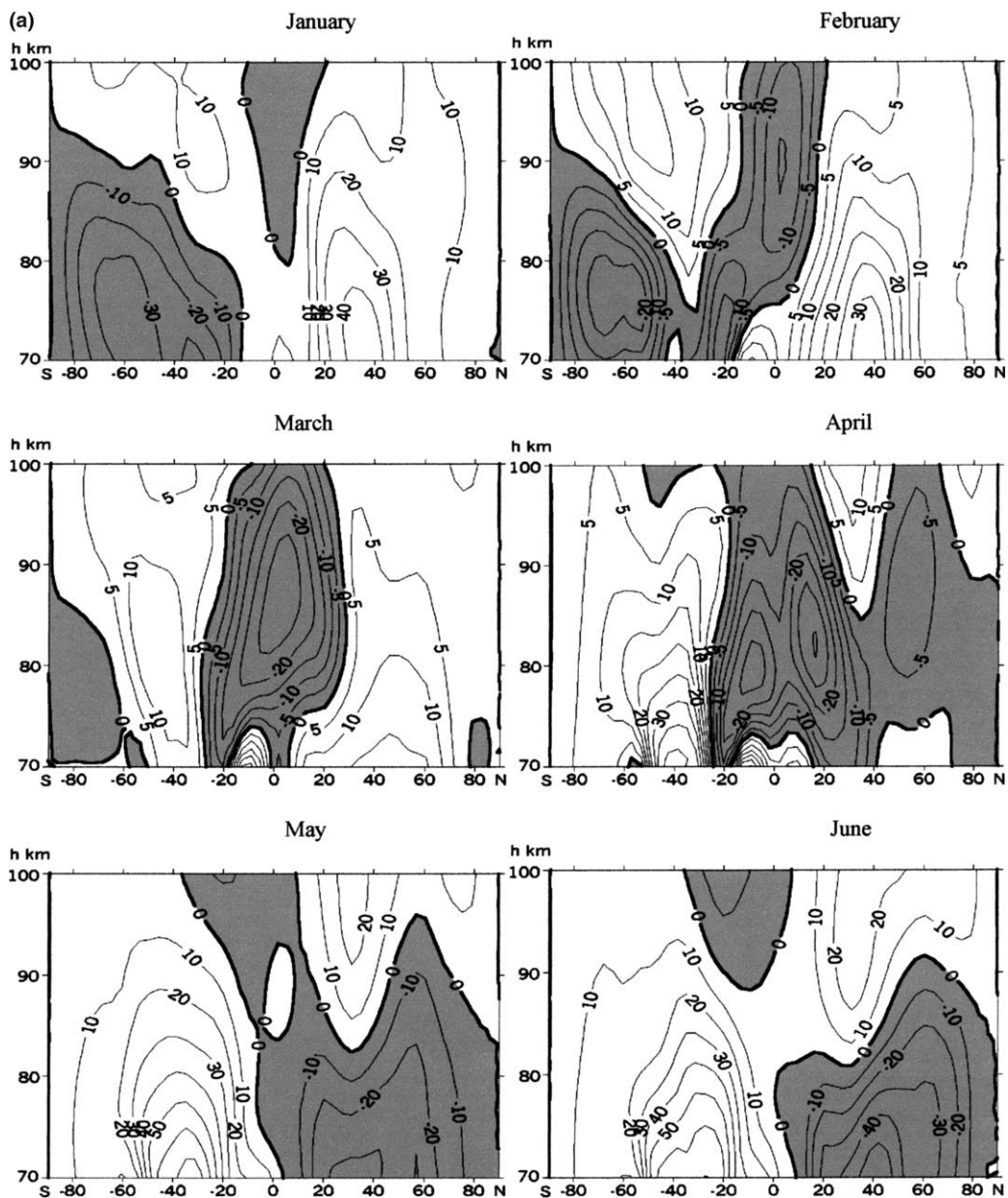


Fig. 2. (a) Height versus latitude contour plots for monthly mean zonal wind (positive eastward); (b) height versus latitude contours plots for monthly mean zonal wind (positive eastward).

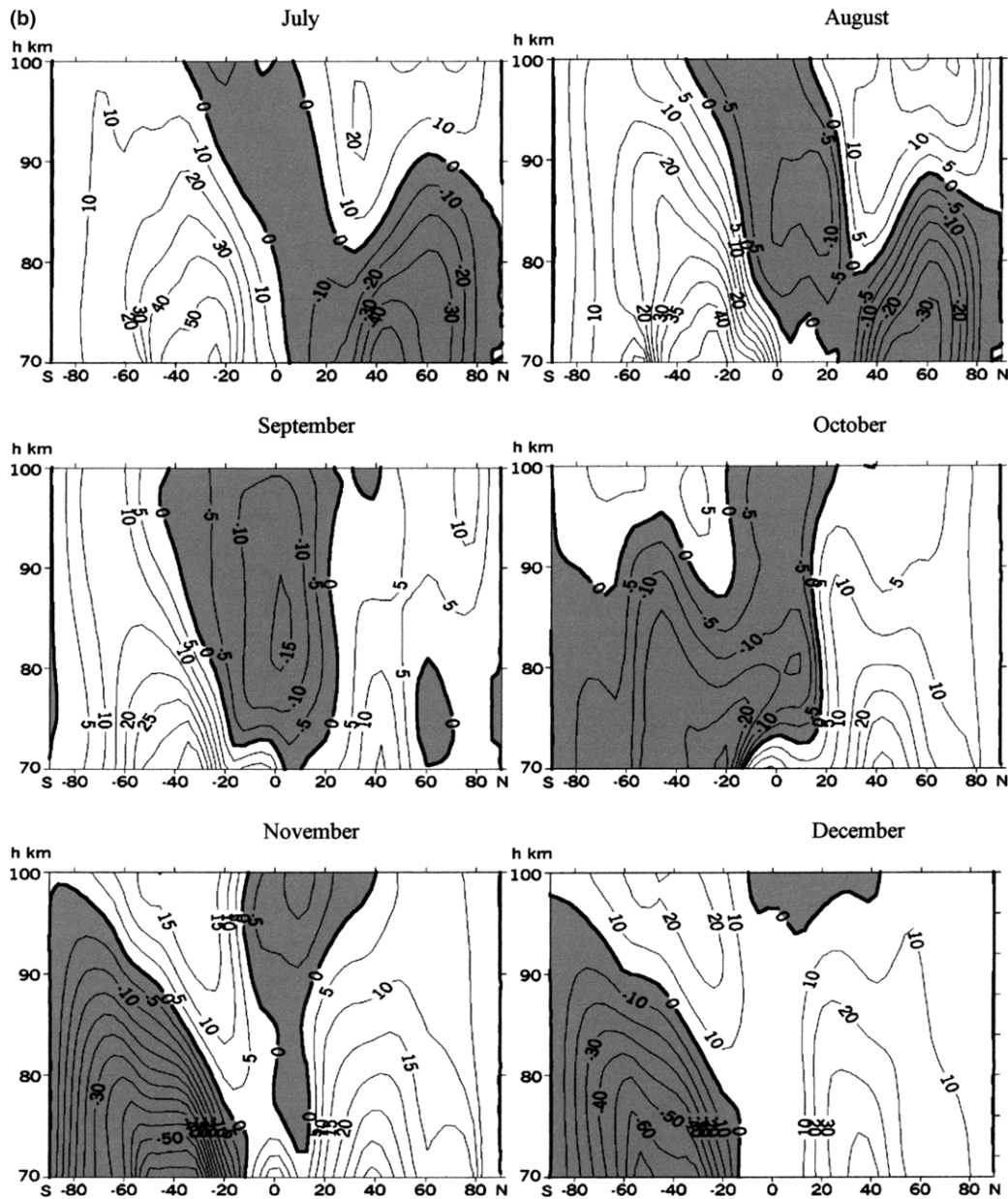


Fig. 2 (continued)

the harmonic fitting over year: the annual mean wind, amplitudes and phases of the annual and semiannual oscillation were calculated and from these values again the monthly mean values were recalculated.

For each ground-based station the monthly mean prevailing wind values at each particular height were averaged over all years of observations. As in the case with the space-based data, the ground-based meridional winds were also smoothed over year, thus the final monthly mean values are the result of superposition of the annual mean wind and the 12- and 6-months oscillations.

The scatter plots in Fig. 1 depict monthly mean zonal (top panel) and meridional prevailing winds (bottom)

from the MF radars (filled circles) and from the meteor radars (open circles) vs. those derived from the HRDI measurements. The solid line represents the least-squares linear fit to these data.

While the GB and SB zonal wind data are obviously well correlated ( $R_{MF} = 0.63$ ,  $R_{MR} = 0.71$ ), the magnitude of prevailing zonal wind sensed by the HRDI instrument is on average 70% higher than that of the radars in addition to  $6 \text{ ms}^{-1}$  net bias for the MR radars and  $4 \text{ ms}^{-1}$  for the MF radars. Because we consider the MR data as the most reliable ones, for constructing of the model from the the HRDI zonal winds constant wind  $6 \text{ ms}^{-1}$  were subtracted and these winds were divided at the factor 1.7, while additionally

$2 \text{ ms}^{-1}$  were added to the MF zonal winds. The resulting scatter plot with the HRDI corrected data is shown in Fig. 1 (middle panel). The bottom panel of Fig. 1 is the same as the upper panel, except for meridional wind. The amplitudes are much smaller and the scatter much larger than for zonal wind and correlation is lower, especially for the MF radars, but still significant. In this case no significant systematic bias between the SB and GB data is found and no correction of the HRDI data is needed.

The obtained GB monthly mean wind values at the all available heights and SB at 96 km were interpolated over height and latitude using the two-dimensional procedure

(McLane, 1972). The optimal weighting function coefficients were found to be:  $\sigma_{\text{lat.}} = 7^\circ$ ,  $\sigma_h = 4.5 \text{ km}$ .

#### 4. Model contour plots

The climatic zonal and meridional wind model contour plots for all months of the year are shown in Figs. 2 and 3. In general, these plots are mainly similar to those described by Portnyagin and Solovjova (2002). So, due to lack of space here we refer to this paper for comprehensive description of the main global wind structures and their seasonal transformations. However in comparison with

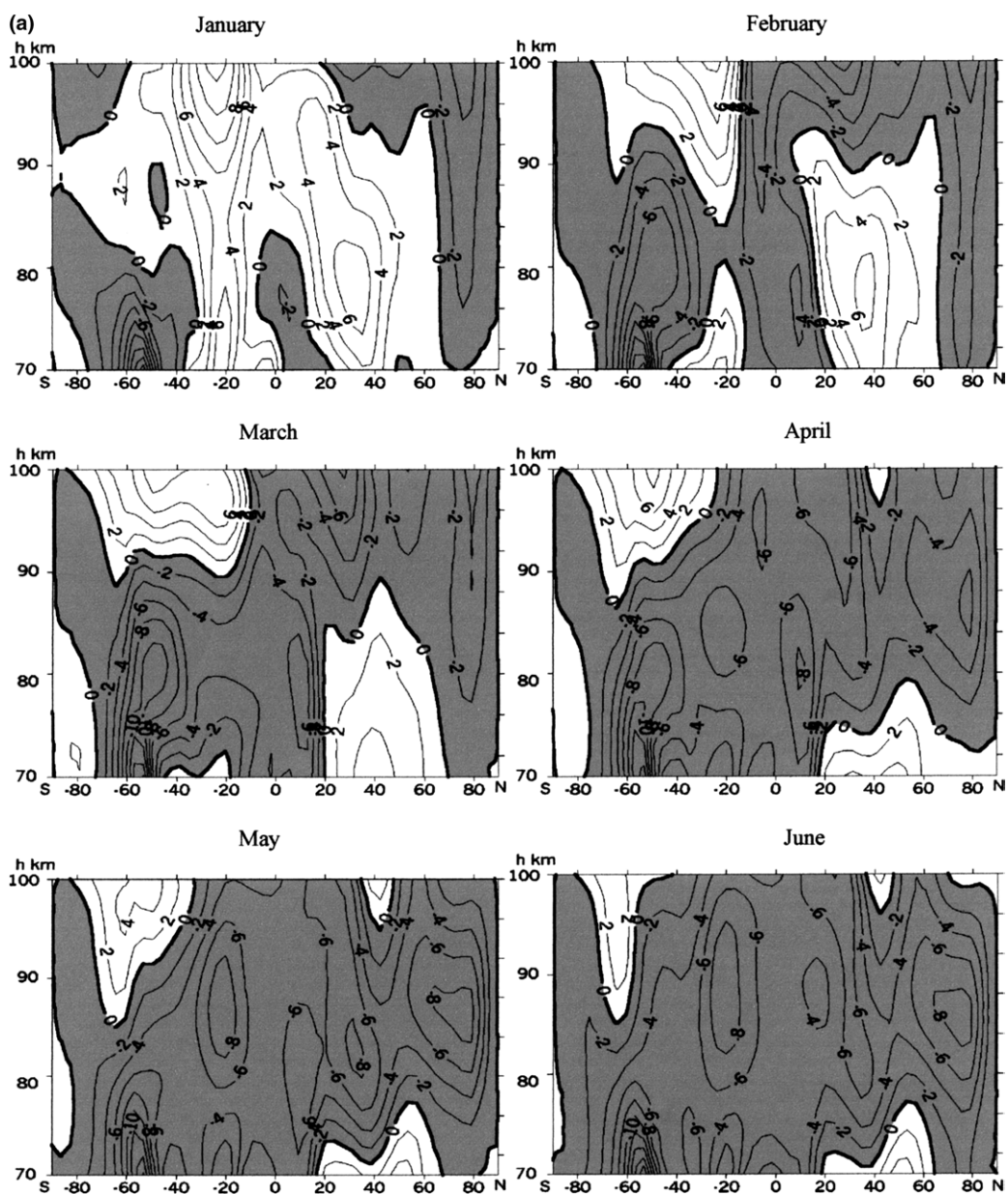


Fig. 3. (a) Height versus latitude contour plots for monthly mean meridional wind (positive northward); (b) height versus latitude contour plots for monthly mean meridional wind (positive northward).

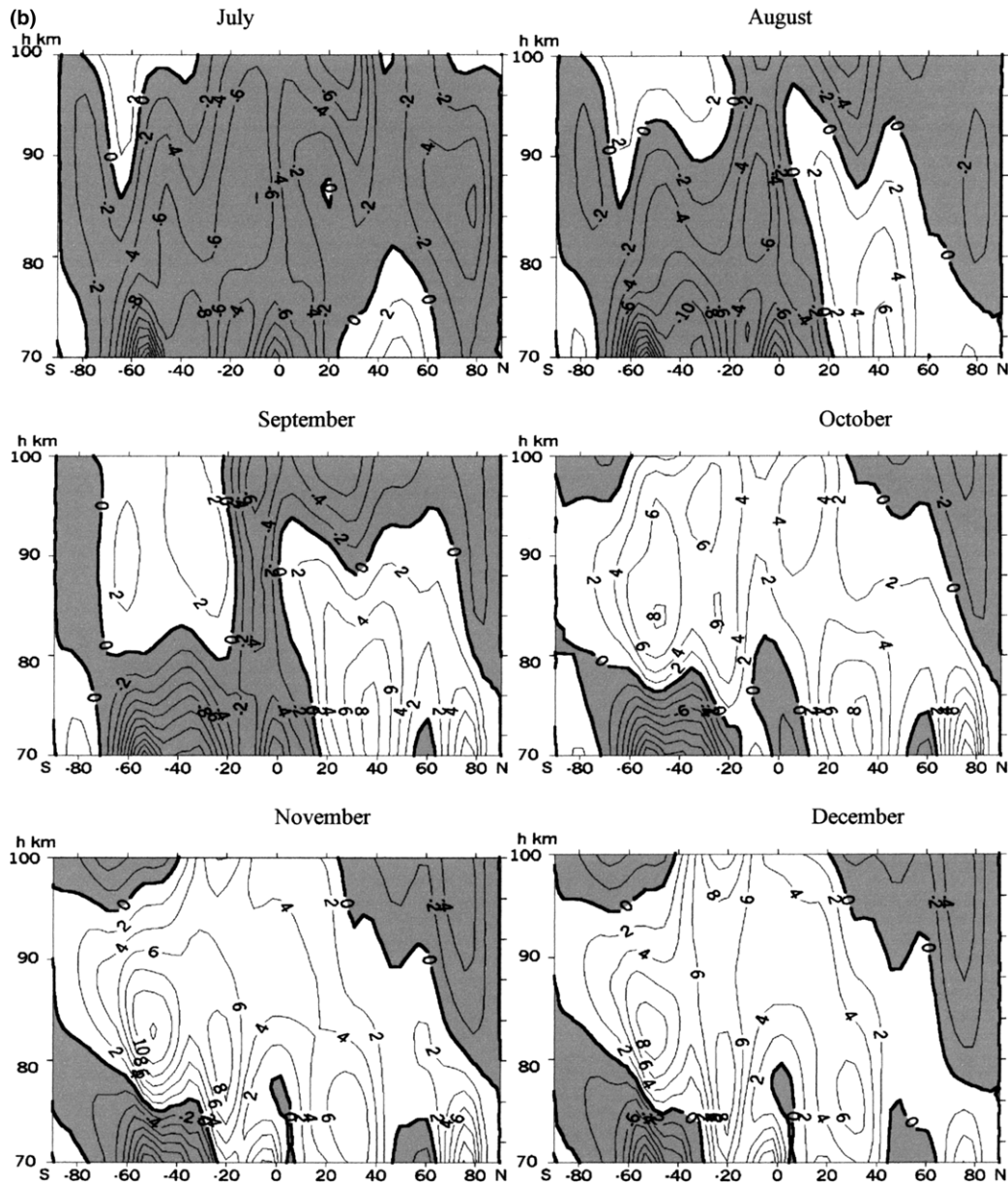


Fig. 3 (continued)

the Portnyagin and Solovjova model the present model is characterized by a rather lower amplitudes of winds in average at a factor 1.5. This is obvious result of more careful averaging of the used more comprehensive datasets. Moreover, in some regions of a relatively weak winds, especially for meridional component, the signs of the winds are different from those described by Portnyagin and Solovjova (2002). As a result, the form and location of the main circulation structures in the present model are different from the earlier models. When comparing of the different models we have to have in mind that the MLT global dynamical structures are not completely zonally symmetric as well as not fully identical from year to year.

## 5. Conclusion

The presented 2-D climatic MLT (70–100 km) prevailing wind model is the first one where the GB and SB data were combined. It is shown that these datasets are well complemented each other when some systematic differences are taken into account. New method of constructing of the model was proposed. The revealed MLT circulation structures are global in nature and regularly change from month to month. Some differences between the present model and the earlier ones are found. The model is available in the computer readable form and may be used for construction of the new CIRA model.

**References**

- Hays, P.B., Abreu, V.J., Dobbs, M.E., et al. The high resolution Doppler imager on the upper atmosphere research satellite. *J. Geophys. Res.* 98 (10), 713–723, 1993.
- McLane, D.H. Drawing contours from arbitrary data points. *Computer J.* 17, 318–324, 1972.
- Portnyagin, Yu.I., Solovjova, T.V. Global empirical model for the upper mesosphere/lower thermosphere. *Ann. Geophysicae* 18, 300–315, 2002.